

One-loop off-shell decay $H^* \rightarrow ZZ$ at future colliders

Khien Hong Phan^{1,2†}, Dzung Tri Tran^{1,2} and Anh Thu Nguyen³

¹*Institute of Fundamental and Applied Sciences, Duy Tan University,
Ho Chi Minh City 700000, Vietnam*

²*Faculty of Natural Sciences, Duy Tan University, Da Nang City 550000, Vietnam*

³*University of Science Ho Chi Minh City,
227 Nguyen Van Cu, District 5, Ho Chi Minh City, Vietnam*

E-mail: [†]phanhongkiem@duytan.edu.vn

Received 17 February 2023; Accepted for publication 12 May 2023; Published 8 December 2023

Abstract. We present one-loop formulas for contributing to the HZZ vertex in 't Hooft-Veltman gauge within Standard Model framework. One-loop off-shell Higgs decay rates to Z-pair are investigated in both unpolarized and longitudinal polarization for Z bosons in final state. The corrections are range of 7% to 8.4% when we vary the off-shell Higgs mass from 200 GeV to 500 GeV. In applications, we study off-shell Higgs decay $H^* \rightarrow ZZ$ in the Higgs productions at future colliders such as the signal processes $\gamma^*(Q^2)\gamma \rightarrow H^* \rightarrow ZZ$ and $e^-\gamma \rightarrow e^-H^* \rightarrow e^-ZZ$ are analyzed.

Keywords: one-loop corrections; analytic methods for quantum field theory; dimensional regularization; Higgs phenomenology.

Classification numbers: 03.70.+k; 11.10.-z.

1. Introduction

Since the discovery of the Standard-Model-like (SM-like) Higgs boson at the Large Hadron Collider (LHC) [1, 2], High energy physics has entered a new era. High-precision measurements of the Higgs properties are the top priority tasks at the LHC. So far, most of the measurements at the LHC focus on the on-shell Higgs productions and on-shell Higgs decay channels. The data shows that the Higgs signal strengths are in agreement with the SM predictions. The above measurements are planned to probe as precisely as possible in near future for the high-precision tests of the SM as well as extracting new physics beyond the SM (BSM). Besides that, in order to explore the nature of Higgs sector at different energy scales, off-shell Higgs decay channels are considerable interests. Recently, off-shell Higgs decay $H^* \rightarrow Z^*Z^* \rightarrow 4$ leptons have been measured at the LHC in Refs. [3–8].

We argue that off-shell Higgs decay channel $H^* \rightarrow ZZ \rightarrow 4$ leptons provides rich of phenomenological investigations. In Ref. [9], examining the tail of off-shell Higgs decay mode $H^* \rightarrow Z_L Z_L$, one can test the unitarity of the SM and explore new physics through high energy behavior. Searching for new physics through off-shell Higgs decay $H^* \rightarrow ZZ \rightarrow l^+ l^- \nu_l \bar{\nu}_l$ has been studied in Ref. [10] in which the authors have considered the effective theory by proposing the energy-dependent operators. Off-Shell Higgs decays as a probe of naturalness have been discussed in Ref. [11] and as a probe of the trilinear Higgs coupling have been reported in Ref. [12]. Through the examination of the decay channel $H \rightarrow ZZ^* \rightarrow 4$ leptons at the LHC, the authors in Ref. [13] have studied the effects of the CP-conserving and CP-violating of the general HZZ coupling. Other phenomenological studies of off-shell Higgs decay in many of BSMs have been found in Refs. [14–20].

At the LHC, one-loop and two-loop QCD corrections for both signal and background of the off-shell Higgs decay $H^* \rightarrow ZZ$ have been computed in [21–30]. One-loop electroweak corrections to Higgs boson decay into ZZ in standard model have been reported in [31], in the minimal supersymmetric model [32, 33], and to Higgs boson decay into four leptons have been evaluated in Refs. [34–36]. Off-shell Higgs decay effects in Higgs productions at future linear colliders have been studied in Refs. [37, 38] in which the authors have included only the tree level vertex HZZ in the analysis. Due to the important roles of the off-shell Higgs decays and in order to match the high-precision data at future colliders, we evaluate for one-loop electroweak corrections to the off-shell decay $H^* \rightarrow ZZ$ in this work. The computation is performed in 't Hooft-Veltman gauge. Analytic formulas for one-loop form factors in the decay process are expressed in terms of Passarino-Veltman scalar functions in the standard notations of `LoopTools`. As a result, the off-shell decay rates can be evaluated numerically by using this package. One-loop electroweak corrections to the off-shell decay rates are studied for the cases of unpolarized Z bosons and longitudinal polarization of Z bosons in final state. In applications, we study off-shell Higgs decay $H^* \rightarrow ZZ$ in the Higgs productions at future colliders such as the signal processes $\gamma^*(Q^2)\gamma \rightarrow H^* \rightarrow ZZ$ and $e^- \gamma \rightarrow e^- H^* \rightarrow e^- ZZ$ are analyzed.

The layout of the paper is as follows: In section 2, we present one-loop expressions for the vertex HZZ . Phenomenological results for this work are shown in the section 3. Conclusions and outlook for this research are discussed in the section 4.

2. Calculations

In general, one-loop contributions to the $H(p)Z(q_1)Z(q_2)$ vertex are decomposed in terms of Lorentz structure as follows:

$$\mathcal{V}_{HZZ}^{1\text{-loop}}(p, q_1, q_2) = g_{HZZ} \left(F_{00} g^{\mu\nu} + \sum_{i,j=1}^2 F_{ij} q_i^\mu q_j^\nu \right). \quad (1)$$

The tree level coupling of the Higgs to ZZ is given $g_{HZZ} = \frac{eM_W}{c_W^2 s_W}$ where s_W and c_W are sine and cosine of Weinberg angle respectively. In this expression, the terms F_{00} , F_{ij} for $i, j = 1, 2$ are denoted for one-loop form factors. These form factors are functions of p^2, q_1^2, q_2^2 and they are expressed in terms of Passarino-Veltman scalar functions (called as PV-functions hereafter). All one-loop Feynman diagrams contributing to this vertex can be grouped into three classes as follows (shown in appendix D). By considering all fermions exchanging in the loop diagrams, this is corresponding to group 1. With including all W bosons, goldstone bosons and ghost particles

propagating in the loop, we have group 2 accordingly. One finally takes Z boson, Higgs and goldstone bosons exchanging in the loop, we have correspondingly to group 3. It is known that one-loop contributing to the vertex HZZ contains ultraviolet divergent (UV -divergent). Following renormalization theory, the counter-terms are given for cancelling the UV -divergent. We then have counter-term diagrams in group 0 whose analytic formulas are presented in appendix C.

Analytic results for the above form factors are computed class by class of Feynman diagrams as follows. First, one-loop amplitudes for all Feynman diagrams mentioned above are written down. We then handle with Dirac traces and Lorentz contractions in d dimensions by using Package-X [39]. The amplitudes are next decomposed into tensor one-loop integrals. By following tensor reduction for one-loop integrals in [40], the tensor integrals are then expressed in terms of the PV-functions, which can be evaluated numerically by using LoopTools [41]. In detail, analytical results for all form factors are shown in the following paragraphs. General expression for the form factor $F_{00}(p^2; q_1^2, q_2^2)$ is written as follows:

$$F_{00}(p^2; q_1^2, q_2^2) = \sum_{G=\{G_0, G_1, \dots, G_3\}} F_{00}^{(G)}(p^2; q_1^2, q_2^2). \quad (2)$$

where $\{G_0, G_1, \dots, G_3\} = \{\text{group 0, group 1} \dots, \text{group 3}\}$ are groups of Feynman diagrams showing in appendix D. The form factor $F_{00}^{(G_0)}(p^2; q_1^2, q_2^2)$ for group 0 is expressed in the appendix C. In group 1, we consider all fermions exchanging in the loop. We take top quark in the loop for an example. The resulting for the form factor reads:

$$\begin{aligned} F_{00}^{(G_1)}(p^2; q_1^2, q_2^2) &= \frac{e^3}{576\pi^2 M_W s_W^3 c_W^2} N_t^C m_t^2 \times \quad (3) \\ &\times \left\{ 2(32s_W^4 - 24s_W^2 + 9)B_0(p^2, m_t^2, m_t^2) + 9 \left[B_0(q_1^2, m_t^2, m_t^2) + B_0(q_2^2, m_t^2, m_t^2) \right] \right. \\ &+ \left[36m_t^2 + 8s_W^2(3 - 4s_W^2)(-p^2 + q_1^2 + q_2^2) - 9(q_1^2 + q_2^2) \right] C_0(p^2, q_1^2, q_2^2, m_t^2, m_t^2, m_t^2) \\ &\left. - 8(32s_W^4 - 24s_W^2 + 9)C_{00}(p^2, q_1^2, q_2^2, m_t^2, m_t^2, m_t^2) \right\}. \end{aligned}$$

Here $N_t^C = 3$ is color number top quark. For group 2, we take into account all W bosons in the loop diagrams. The form factor is then given:

$$\begin{aligned} F_{00}^{(G_2)}(p^2; q_1^2, q_2^2) &= \frac{e^3}{64\pi^2 M_W s_W^3 c_W^2} \times \left\{ 4M_W^2 (c_W^4 - s_W^4) \left[B_0(q_1^2, M_W^2, M_W^2) + B_0(q_2^2, M_W^2, M_W^2) \right] \quad (4) \right. \\ &- 4M_W^2 \left[c_W^4 (5p^2 - 4(q_1^2 + q_2^2 + M_W^2)) + s_W^2 c_W^2 (q_1^2 + q_2^2 - 2(p^2 + M_W^2)) + s_W^4 (2M_W^2 + M_H^2) \right] \\ &\quad \times C_0(p^2, q_1^2, q_2^2, M_W^2, M_W^2, M_W^2) \\ &+ \left[4M_H^2 (c_W^2 - s_W^2)^2 + 8M_W^2 (c_W^4 (4d - 7) - 2c_W^2 s_W^2 + s_W^4) \right] \times C_{00}(p^2, q_1^2, q_2^2, M_W^2, M_W^2, M_W^2) \\ &\left. - \left[8M_W^2 c_W^2 (c_W^2 (d - 2) - s_W^2) + M_H^2 (c_W^2 - s_W^2)^2 \right] B_0(p^2, M_W^2, M_W^2) \right\}. \end{aligned}$$

We next consider the contributions from group 3 in which the particles Z, χ_3, H are exchanged in the loop diagrams. The form factor is evaluated accordingly:

$$\begin{aligned}
F_{00}^{(G_3)}(p^2; q_1^2, q_2^2) &= -\frac{e^3}{128\pi^2 M_W s_W^3 c_W^6} \quad (5) \\
&\times \left\{ 4c_W^2 M_W^2 \left[B_0(q_1^2, M_H^2, M_Z^2) + B_0(q_2^2, M_H^2, M_Z^2) + 3M_H^2 C_0(p^2, q_1^2, q_2^2, M_H^2, M_H^2, M_Z^2) \right] \right. \\
&+ M_H^2 c_W^4 B_0(p^2, M_Z^2, M_Z^2) + 3c_W^4 M_H^2 B_0(p^2, M_H^2, M_H^2) \\
&+ 8M_W^4 C_0(p^2, q_1^2, q_2^2, M_Z^2, M_Z^2, M_H^2) - 12M_H^2 c_W^4 C_{00}(p^2, q_1^2, q_2^2, M_H^2, M_H^2, M_Z^2) \\
&\left. - 4c_W^2 (c_W^2 M_H^2 + 2M_W^2) C_{00}(p^2, q_1^2, q_2^2, M_Z^2, M_Z^2, M_H^2) \right\}.
\end{aligned}$$

Other form factors (F_{ij} for $i, j = 1, 2$) are also written in the form of

$$F_{ij}(p^2; q_1^2, q_2^2) = \sum_{G=\{G_1, \dots, G_3\}} F_{ij}^{(G)}(p^2; q_1^2, q_2^2). \quad (6)$$

All form factors F_{ij} for $i, j = 1, 2$ are the UV-finite. Therefore, we have only group 1 to group 3 contributing to these form factors. Applying the same procedure, each form factor is expressed as follows:

$$\begin{aligned}
F_{11}^{(G_1)}(p^2; q_1^2, q_2^2) &= -\frac{e^3(32s_W^4 - 24s_W^2 + 9)}{144\pi^2 M_W s_W^3 c_W^2} N_i^C m_i^2 \times \quad (7) \\
&\times \left[C_1(p^2, q_1^2, q_2^2, m_i^2, m_i^2, m_i^2) + 2C_{11}(p^2, q_1^2, q_2^2, m_i^2, m_i^2, m_i^2) \right],
\end{aligned}$$

$$\begin{aligned}
F_{11}^{(G_2)}(p^2; q_1^2, q_2^2) &= \frac{e^3}{32\pi^2 M_W s_W^3 c_W^2} \times \quad (8) \\
&\times \left\{ \left[M_H^2 (c_W^2 - s_W^2)^2 + M_W^2 \left(2c_W^4 (4d - 7) - 3c_W^2 s_W^2 + 3s_W^4 \right) \right] \times \right. \\
&\quad \times C_1(p^2, q_1^2, q_2^2, M_W^2, M_W^2, M_W^2) \\
&+ \left[2M_H^2 (c_W^2 - s_W^2)^2 + 4M_W^2 \left(c_W^4 (4d - 7) - 2c_W^2 s_W^2 + s_W^4 \right) \right] \times \\
&\quad \times C_{11}(p^2, q_1^2, q_2^2, M_W^2, M_W^2, M_W^2) \\
&\left. + 2M_W^2 s_W^2 (s_W^2 - 2c_W^2) C_0(p^2, q_1^2, q_2^2, M_W^2, M_W^2, M_W^2) \right\},
\end{aligned}$$

$$\begin{aligned}
 F_{11}^{(G_3)}(p^2; q_1^2, q_2^2) &= \frac{e^3}{64\pi^2 M_W s_W^3 c_W^4} \left\{ 2M_W^2 C_0(p^2, q_1^2, q_2^2, M_Z^2, M_Z^2, M_H^2) \right. \\
 &+ (c_W^2 M_H^2 + 3M_W^2) C_1(p^2, q_1^2, q_2^2, M_Z^2, M_Z^2, M_H^2) \\
 &+ 3c_W^2 M_H^2 \left[C_1(p^2, q_1^2, q_2^2, M_H^2, M_H^2, M_Z^2) + 2C_{11}(p^2, q_1^2, q_2^2, M_H^2, M_H^2, M_Z^2) \right] \\
 &\left. + 2(c_W^2 M_H^2 + 2M_W^2) C_{11}(p^2, q_1^2, q_2^2, M_Z^2, M_Z^2, M_H^2) \right\}. \tag{9}
 \end{aligned}$$

Analytic results for the form factors F_{12} are shown as:

$$\begin{aligned}
 F_{12}^{(G_1)}(p^2; q_1^2, q_2^2) &= -\frac{e^3}{288\pi^2 M_W s_W^3 c_W^2} N_t^C m_t^2 \left\{ 8s_W^2 (3 - 4s_W^2) C_0(p^2, q_1^2, q_2^2, m_t^2, m_t^2, m_t^2) \right. \\
 &- (3 - 8s_W^2)^2 \left[C_1(p^2, q_1^2, q_2^2, m_t^2, m_t^2, m_t^2) + C_1(p^2, q_2^2, q_1^2, m_t^2, m_t^2, m_t^2) \right] \\
 &\left. - 4(32s_W^4 - 24s_W^2 + 9) C_{12}(q_1^2, p^2, q_2^2, m_t^2, m_t^2, m_t^2) \right\}, \tag{10}
 \end{aligned}$$

$$\begin{aligned}
 F_{12}^{(G_2)}(p^2; q_1^2, q_2^2) &= \frac{e^3}{64\pi^2 M_W s_W^3 c_W^2} \left\{ \left[4M_W^2 (3s_W^2 c_W^2 + s_W^4 - 2c_W^4 (d - 2)) - M_H^2 (c_W^2 - s_W^2)^2 \right] \right. \\
 &\quad \times C_0(p^2, q_1^2, q_2^2, M_W^2, M_W^2, M_W^2) \\
 &+ \left[M_H^2 (c_W^2 - s_W^2)^2 + M_W^2 (2c_W^4 (4d - 9) - 11c_W^2 s_W^2 - s_W^4) \right] \times \\
 &\quad \times \left[C_1(p^2, q_2^2, q_1^2, M_W^2, M_W^2, M_W^2) - 2C_1(p^2, q_1^2, q_2^2, M_W^2, M_W^2, M_W^2) \right] \\
 &- 4 \left[M_H^2 (c_W^2 - s_W^2)^2 + 2M_W^2 (c_W^4 (4d - 7) - 2s_W^2 c_W^2 + s_W^4) \right] \\
 &\quad \left. \times C_{12}(q_1^2, p^2, q_2^2, M_W^2, M_W^2, M_W^2) \right\}, \tag{11}
 \end{aligned}$$

$$\begin{aligned}
 F_{12}^{(G_3)}(p^2; q_1^2, q_2^2) &= \frac{e^3}{128\pi^2 M_W s_W^3 c_W^4} \left\{ (4M_W^2 - c_W^2 M_H^2) C_0(p^2, q_1^2, q_2^2, M_Z^2, M_Z^2, M_H^2) \right. \\
 &- 3c_W^2 M_H^2 C_0(p^2, q_1^2, q_2^2, M_H^2, M_H^2, M_Z^2) \\
 &- 6c_W^2 M_H^2 \left[C_1(p^2, q_1^2, q_2^2, M_H^2, M_H^2, M_Z^2) + C_1(p^2, q_2^2, q_1^2, M_H^2, M_H^2, M_Z^2) \right. \\
 &\quad \left. + 2C_{12}(q_1^2, p^2, q_2^2, M_Z^2, M_H^2, M_H^2) \right] \\
 &+ (2M_W^2 - 2c_W^2 M_H^2) \left[C_1(p^2, q_1^2, q_2^2, M_Z^2, M_Z^2, M_H^2) + C_1(p^2, q_2^2, q_1^2, M_Z^2, M_Z^2, M_H^2) \right] \\
 &\left. - 4(2M_W^2 + c_W^2 M_H^2) C_{12}(q_1^2, p^2, q_2^2, M_H^2, M_Z^2, M_Z^2) \right\}. \tag{12}
 \end{aligned}$$

We list all analytic expressions for the form factor F_{21} as follows:

$$F_{21}^{(G_1)}(p^2; q_1^2, q_2^2) = -\frac{e^3}{288\pi^2 M_W s_W^3 c_W^2} N_t^C m_t^2 \times \quad (13)$$

$$\times \left\{ 8s_W^2 (4s_W^2 - 3) C_0(p^2, q_1^2, q_2^2, m_t^2, m_t^2, m_t^2) - 9 \left[C_1(p^2, q_1^2, q_2^2, m_t^2, m_t^2, m_t^2) \right. \right.$$

$$\left. \left. + C_1(p^2, q_2^2, q_1^2, m_t^2, m_t^2, m_t^2) \right] - 4(32s_W^4 - 24s_W^2 + 9) C_{12}(q_1^2, p^2, q_2^2, m_t^2, m_t^2, m_t^2) \right\},$$

$$F_{21}^{(G_2)}(p^2; q_1^2, q_2^2) = -\frac{e^3}{16\pi^2 M_W s_W^3 c_W^2} \left\{ \left[M_H^2 (c_W^2 - s_W^2)^2 + 2M_W^2 (c_W^4 (4d - 7) + s_W^2 (s_W^2 - 2c_W^2)) \right] \right.$$

$$\times C_{12}(q_1^2, p^2, q_2^2, M_W^2, M_W^2, M_W^2)$$

$$\left. + 2M_W^2 \left[C_1(p^2, q_1^2, q_2^2, M_W^2, M_W^2, M_W^2) + C_1(p^2, q_2^2, q_1^2, M_W^2, M_W^2, M_W^2) \right] \right.$$

$$\left. + 8M_W^2 c_W^2 (s_W^2 - c_W^2) C_0(p^2, q_1^2, q_2^2, M_W^2, M_W^2, M_W^2) \right\}, \quad (14)$$

$$F_{21}^{(G_3)}(p^2; q_1^2, q_2^2) = -\frac{e^3}{32\pi^2 M_W s_W^3 c_W^4} \times$$

$$\times \left\{ 2M_W^2 \left[C_1(p^2, q_1^2, q_2^2, M_Z^2, M_Z^2, M_H^2) + C_1(p^2, q_2^2, q_1^2, M_Z^2, M_Z^2, M_H^2) \right] \right.$$

$$\left. + (c_W^2 M_H^2 + 2M_W^2) C_{12}(q_1^2, p^2, q_2^2, M_H^2, M_Z^2, M_Z^2) \right.$$

$$\left. + 3c_W^2 M_H^2 C_{12}(q_1^2, p^2, q_2^2, M_Z^2, M_H^2, M_H^2) \right\}. \quad (15)$$

The last form factor F_{22} can be derived directly as

$$F_{22}(p^2; q_1^2, q_2^2) = F_{11}(p^2; q_2^2, q_1^2). \quad (16)$$

Moreover, it is easy to check that all form factors satisfy the Bose symmetry relations

$$F_{00,12,21}(p^2; q_1^2, q_2^2) = F_{00,12,21}(p^2; q_2^2, q_1^2). \quad (17)$$

We turn our attention to one-loop amplitude for off-shell $H^* \rightarrow ZZ$. In this case, we only have F_{00}, F_{21} contributing to the amplitude. Analytic expressions for these form factors can be obtained by taking $q_1^2 = q_2^2 = M_Z^2$. One-loop off-shell decay rates for $H^* \rightarrow ZZ, Z_L Z_L$ are computed. We use the following kinematic variables: $p^2 = M_{ZZ}^2, q_1^2 = M_Z^2$ and $q_2^2 = M_Z^2$. Decay rate for the

case of unpolarized Z bosons in final state gets the form of

$$\begin{aligned} \Gamma_{H^* \rightarrow ZZ} = & \frac{g_{HZZ}^2 \sqrt{\lambda(M_{ZZ}^2, M_Z^2, M_Z^2)}}{(64\pi)M_Z^4 M_{ZZ}^3} \left\{ \left(12M_Z^4 - 4M_Z^2 M_{ZZ}^2 + M_{ZZ}^4 \right) + \right. \\ & + \left(2M_{ZZ}^4 - 8M_Z^2 M_{ZZ}^2 + 24M_Z^4 \right) \mathcal{R}e \left[F_{00}(M_{ZZ}^2, M_Z^2, M_Z^2) \right] \\ & \left. + \left(8M_Z^4 M_{ZZ}^2 - 6M_Z^2 M_{ZZ}^4 + M_{ZZ}^6 \right) \mathcal{R}e \left[F_{21}(M_{ZZ}^2, M_Z^2, M_Z^2) \right] \right\}. \end{aligned} \quad (18)$$

Here, the Källén function is defined as $\lambda(x; y, z) = (x - y - z)^2 - 4yz$.

We next consider the polarized Z bosons. In rest frame of Higgs boson, the longitudinal polarization vectors for Z bosons are defined as:

$$\varepsilon_\mu(q_i, \lambda = 0) = \frac{4M_{ZZ}^2 q_{i,\mu} - 2M_Z^2 p_\mu}{M_Z \sqrt{\lambda(4M_{ZZ}^2, M_Z^2, M_Z^2)}}, \quad \text{for } i = 1, 2. \quad (19)$$

By deriving again the squared amplitude for off-shell decay $H^* \rightarrow Z_L Z_L$, we then arrive at

$$\begin{aligned} \Gamma_{H^* \rightarrow Z_L Z_L} = & \frac{g_{HZZ}^2 \sqrt{\lambda(M_{ZZ}^2, M_Z^2, M_Z^2)}}{(2\pi)M_Z^4 M_{ZZ}^3 \lambda^2(4M_{ZZ}^2, M_Z^2, M_Z^2)} \left\{ 2M_{ZZ}^4 \left(M_Z^4 - 6M_Z^2 M_{ZZ}^2 + 2M_{ZZ}^4 \right)^2 + \right. \\ & + M_{ZZ}^4 \left(M_Z^4 - 6M_Z^2 M_{ZZ}^2 + 2M_{ZZ}^4 \right) \times \\ & \times \left[\left(4M_Z^4 - 24M_Z^2 M_{ZZ}^2 + 8M_{ZZ}^4 \right) \mathcal{R}e \left[F_{00}(M_{ZZ}^2, M_Z^2, M_Z^2) \right] \right. \\ & \left. \left. + \left(25M_Z^4 M_{ZZ}^2 - 20M_Z^2 M_{ZZ}^4 + 4M_{ZZ}^6 \right) \mathcal{R}e \left[F_{21}(M_{ZZ}^2, M_Z^2, M_Z^2) \right] \right] \right\}. \end{aligned} \quad (20)$$

3. Phenomenological results

In the phenomenological results, we use $M_Z = 91.1876$ GeV, $\Gamma_Z = 2.4952$ GeV, $M_W = 80.379$ GeV, $\Gamma_W = 2.085$ GeV, $M_H = 125$ GeV, $\Gamma_H = 4.07 \cdot 10^{-3}$ GeV. The lepton masses are given: $m_e = 0.00052$ GeV, $m_\mu = 0.10566$ GeV and $m_\tau = 1.77686$ GeV. For quark masses, one takes $m_u = 0.00216$ GeV, $m_d = 0.0048$ GeV, $m_c = 1.27$ GeV, $m_s = 0.93$ GeV, $m_t = 173.0$ GeV, and $m_b = 4.18$ GeV. We work in the so-called G_μ -scheme in which the Fermi constant is taken $G_\mu = 1.16638 \cdot 10^{-5}$ GeV⁻² and the electroweak coupling can be calculated appropriately as follows:

$$\alpha = \sqrt{2}/\pi G_\mu M_W^2 (1 - M_W^2/M_Z^2) = 1/132.184. \quad (21)$$

We then present the phenomenological results in the following subsections. In Fig. 1, off-shell Higgs decay rates as a function of M_{ZZ} are shown. We vary M_{ZZ} from 200 GeV to 500 GeV. In the left (right) panel of Fig. 1, the decay rates are generated in the region of $200 \leq M_{ZZ} \leq 500$ GeV (and zoom out in $200 \leq M_{ZZ} \leq 300$ GeV to study the effects of $H^* \rightarrow Z_L Z_L$), respectively. In these figures, the solid line presents for tree-level decay rates, the dashed line shows for full

one-loop electroweak decay rates. While the dash-dotted line is for full one-loop decay rates with the longitudinal polarization for Z bosons. We find that the decay rates in $H^* \rightarrow Z_L Z_L$ give small contributions in the low region of M_{ZZ} and they tend to one-loop decay rates in high region of M_{ZZ} .

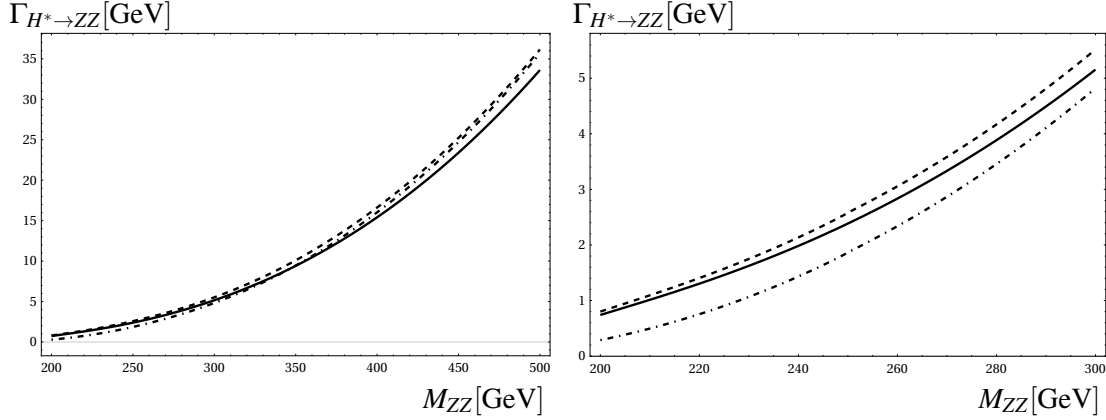


Fig. 1. Off-shell Higgs decay rates as a function of M_{ZZ} .

In Fig. 2, we show one-loop electroweak corrections to the decay rates. The corrections are defined as follows:

$$\delta[\%] = \frac{\Gamma_{H^* \rightarrow ZZ}^{\text{one-loop}} - \Gamma_{H^* \rightarrow ZZ}^{\text{tree}}}{\Gamma_{H^* \rightarrow ZZ}^{\text{tree}}} \times 100\%. \quad (22)$$

In the left panel, one presents one-loop corrections for the case of unpolarized bosons in final state. While the right figure shows for one-loop electroweak corrections for the case of longitudinal polarization for both Z bosons. We find that the corrections are in range of 7% to 8.4% for the case of unpolarized bosons. While the corrections change from -60% to $+10\%$ in the case of longitudinal polarization for both Z bosons. The effects of one-loop electroweak corrections to off-shell Higgs decay $H^* \rightarrow ZZ$ are significant and they should be taken into account at future colliders.

We study the effects of one-loop off-shell $H^* \rightarrow ZZ$ in Higgs productions at future colliders. The first signal process is $\gamma(Q^2)\gamma \rightarrow H^* \rightarrow ZZ$. The signal cross section is given by

$$\sigma(\sqrt{s}, Q^2) = \frac{2\sqrt{s} \Gamma_{H^* \rightarrow ZZ}}{[(s - M_H^2)^2 + \Gamma_H^2 M_H^2] \sqrt{\lambda(s, Q^2, 0)}} \left| F_{00}^{H^* \rightarrow \gamma^* \gamma}(s, Q^2, 0) \right|^2. \quad (23)$$

Where $F_{00}^{H^* \rightarrow \gamma^* \gamma}(s, Q^2, 0)$ is one-loop form factor for process $H^* \rightarrow \gamma^*(Q^2)\gamma$, whose analytical result can be found in [46]. In Fig. 3, total cross sections are plotted as a function of center-of-mass energy (C.o.M) for $Q^2 = 0$ (left panel) and $Q^2 = 1.5M_H^2$ (right panel) respectively. In these Figures, the solid line shows for tree-level cross sections, the dashed line is for one-loop contributing to $H^* \rightarrow ZZ$ and the dash-dotted line presents for one-loop contributing to $H^* \rightarrow Z_L Z_L$.

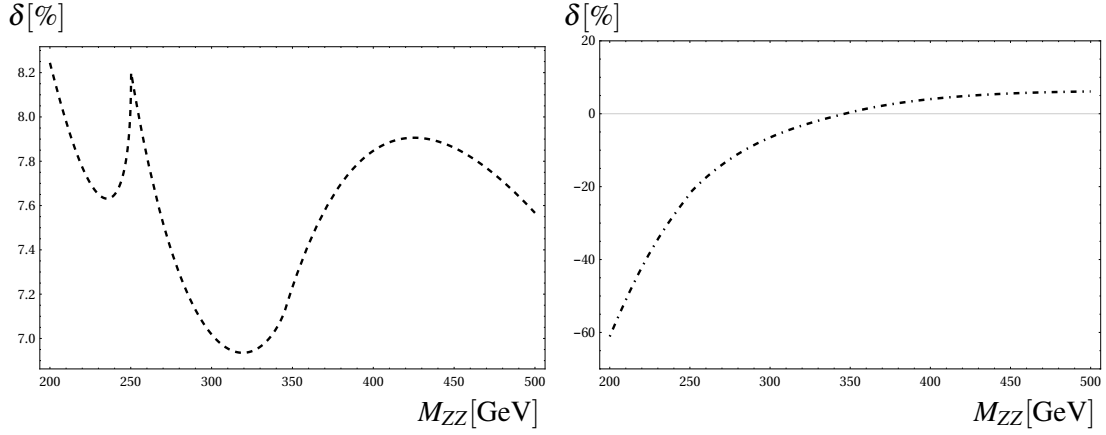


Fig. 2. One-loop electroweak corrections to the decay rates as a function of M_{ZZ} .

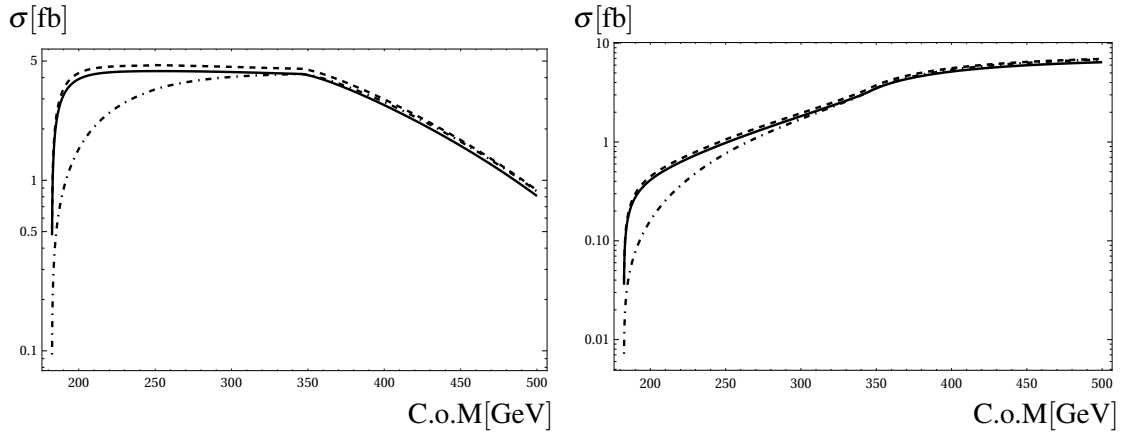


Fig. 3. Total cross sections are plotted as a function of center-of-mass energy (C.o.M) for $Q^2 = 0$ (left panel) and $Q^2 = 1.5M_H^2$ (right panel) respectively.

The second signal process mentioned in this work is $e^- \gamma \rightarrow e^- H^* \rightarrow e^- ZZ$. The signal cross section is written as follows

$$\begin{aligned} \frac{d^2 \sigma(\sqrt{s}, Q^2)}{dM_{ZZ} dQ^2} &= \frac{e^2}{16\pi s} \left[\frac{s^2 + (M_{ZZ}^2 - Q^2 - s)^2}{Q^2 (s^2 - Q^2)^2} \right] \times \left| F_{00}^{H^* \rightarrow \gamma^* \gamma}(s, Q^2, 0) \right|^2 \times \\ &\times \frac{2M_{ZZ}}{[(M_{ZZ}^2 - M_H^2)^2 + \Gamma_H^2 M_H^2]} \times \frac{M_{ZZ} \Gamma_{H^* \rightarrow ZZ}(M_{ZZ})}{\pi}. \end{aligned} \quad (24)$$

In Fig. 4, we present differential cross sections with respect to off-shell Higgs mass M_{ZZ} (left panel) and Q^2 (right panel). In these distributions, we use the same previous notations. In the left Figure, cross section develops to the peak which is corresponding to $M_{ZZ} \sim 2M_Z$. It then decreases rapidly beyond the peak. It is interesting to observe that one-loop off-shell Higgs decay impacts are visible around the peak. In the right Figure, we find that cross section is dominant in the low

Q^2 regions. In both cases, one finds that the effects of one-loop contributions to off-shell Higgs decay to Z -pair are visible and they should be taken into account at future colliders.

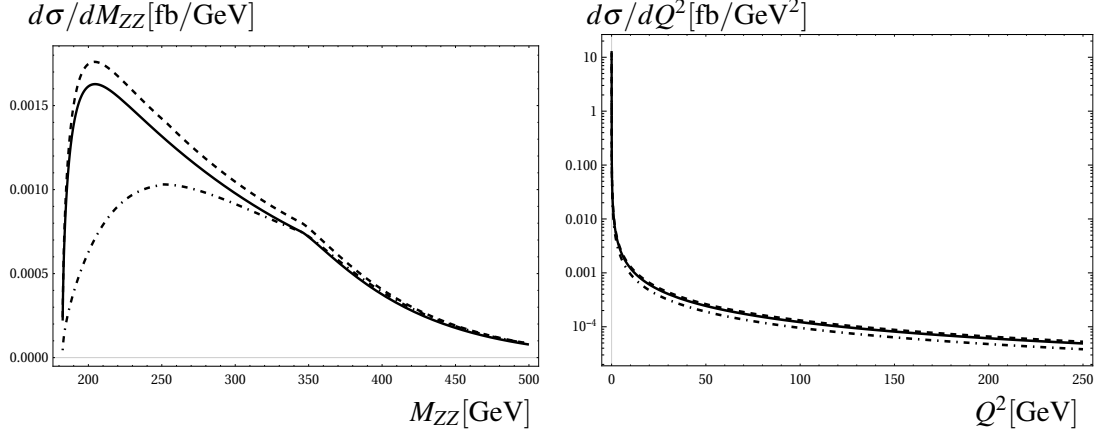


Fig. 4. Differential cross sections are presented as a function of off-shell Higgs mass M_{ZZ} (left panel) and Q^2 (right panel) respectively.

4. Conclusions

In this paper, we have performed one-loop electroweak contributing to HZZ vertex in 't Hooft-Veltman gauge. We have also presented one-loop formulas for off-shell decay $H^* \rightarrow ZZ, Z_L Z_L$. Analytic expressions for one-loop form factors are shown in terms of the PV-functions in the standard notations of LoopTools. Therefore, off-shell decay rates can be computed numerically by using this package. One-loop electroweak corrections to the off-shell decay rates are investigated for the cases of unpolarized Z bosons and longitudinal polarization of Z bosons in final state. The corrections are range of 7% to 8.4% when varying off-shell Higgs mass $200 \text{ GeV} \leq M_{ZZ} \leq 500 \text{ GeV}$. In applications, we study off-shell Higgs decay $H^* \rightarrow ZZ$ in the Higgs productions at future colliders such as the signal processes $\gamma^*(Q^2)\gamma \rightarrow H^* \rightarrow ZZ$ and $e^- \gamma \rightarrow e^- H^* \rightarrow e^- ZZ$ are studied. We find that the effects of one-loop contributions to off-shell Higgs decay to Z -pair are visible and they should be taken into account at future colliders.

Acknowledgment

This research is funded by Vietnam National University, Ho Chi Minh City (VNU-HCM) under grant number C2022-18-14.

References

- [1] ATLAS Collaboration, *Observation of a new particle in the search for the Standard Model Higgs boson with the ATLAS detector at the LHC*, *Phys. Lett. B* **716** (2012) 1.
- [2] CMS Collaboration, *Observation of a New Boson at a Mass of 125 GeV with the CMS Experiment at the LHC*, *Phys. Lett. B* **716** (2012) 30.
- [3] CMS Collaboration, *Constraints on the Higgs boson width from off-shell production and decay to Z-boson pairs*, *Phys. Lett. B* **736** (2014) 64.
- [4] ATLAS Collaboration, *Constraints on the off-shell Higgs boson signal strength in the high-mass ZZ and WW final states with the ATLAS detector*, *Eur. Phys. J. C* **75** (2015) 335.

- [5] ATLAS Collaboration, *Search for an additional, heavy Higgs boson in the $H \rightarrow ZZ$ decay channel at $\sqrt{s} = 8$ TeV in pp collision data with the ATLAS detector*, *Eur. Phys. J. C* **76** (2016) 45.
- [6] ATLAS Collaboration, *Constraints on off-shell Higgs boson production and the Higgs boson total width in $ZZ \rightarrow 4\ell$ and $ZZ \rightarrow 2\ell 2\nu$ final states with the ATLAS detector*, *Phys. Lett. B* **786** (2018) 223.
- [7] CMS Collaboration, *Measurements of the Higgs boson width and anomalous HVV couplings from on-shell and off-shell production in the four-lepton final state*, *Phys. Rev. D* **99** (2019) no.11, 112003.
- [8] CMS Collaboration, *Evidence for off-shell Higgs boson production and first measurement of its width*, CMS-PAS-HIG-21-013.
- [9] S. J. Lee, M. Park and Z. Qian, *Probing unitarity violation in the tail of the off-shell Higgs boson in $V_L V_L$ mode*, *Phys. Rev. D* **100** (2019) 011702.
- [10] D. Gonçalves, T. Han, S. Ching Iris Leung and H. Qin, *Off-shell Higgs couplings in $H^* \rightarrow ZZ \rightarrow \ell\ell\nu\nu$* , *Phys. Lett. B* **817** (2021) 136329.
- [11] D. Gonçalves, T. Han and S. Mukhopadhyay, *Off-Shell Higgs Probe of Naturalness*, *Phys. Rev. Lett.* **120** (2018) 111801 [erratum: *Phys. Rev. Lett.* **121** (2018) no.7, 079902].
- [12] U. Haisch and G. Koole, *Off-shell Higgs production at the LHC as a probe of the trilinear Higgs coupling*, *JHEP* **02** (2022) 030.
- [13] R. M. Godbole, D. J. Miller and M. M. Muhlleitner, *Aspects of CP violation in the $H ZZ$ coupling at the LHC*, *JHEP* **12** (2007) 031.
- [14] A. Azatov, J. de Blas, A. Falkowski, A. V. Gritsan, C. Grojean, L. Kang, *et al.* *Off-shell Higgs Interpretations Task Force: Models and Effective Field Theories Subgroup Report*, [arXiv:2203.02418](https://arxiv.org/abs/2203.02418)
- [15] G. Cacciapaglia, A. Deandrea, G. Drieu La Rochelle and J. B. Flament, *Higgs couplings: disentangling New Physics with off-shell measurements*, *Phys. Rev. Lett.* **113** (2014) 201802
- [16] H. E. Logan, *Hiding a Higgs width enhancement from off-shell $gg(\rightarrow h^*)\rightarrow ZZ$ measurements*, *Phys. Rev. D* **92** (2015) 075038.
- [17] C. Englert, Y. Soreq and M. Spannowsky, *Off-Shell Higgs Coupling Measurements in BSM scenarios*, *JHEP* **05** (2015) 145.
- [18] Y. Chen, R. Harnik and R. Vega-Morales, *New opportunities in $h \rightarrow 4\ell$* , *JHEP* **09** (2015) 185.
- [19] D. Gonçalves, T. Han and S. Mukhopadhyay, *Higgs Couplings at High Scales*, *Phys. Rev. D* **98** (2018) 015023.
- [20] S. Dwivedi, D. K. Ghosh, B. Mukhopadhyaya and A. Shivaji, *Distinguishing CP-odd couplings of the Higgs boson to weak boson pairs*, *Phys. Rev. D* **93** (2016) 115039.
- [21] F. Caola, J. M. Henn, K. Melnikov, A. V. Smirnov and V. A. Smirnov, *Two-loop helicity amplitudes for the production of two off-shell electroweak bosons in gluon fusion*, *JHEP* **06** (2015) 129.
- [22] F. Caola, K. Melnikov, R. Röntsch and L. Tancredi, *QCD corrections to ZZ production in gluon fusion at the LHC*, *Phys. Rev. D* **92** (2015) 094028.
- [23] J. M. Campbell, R. K. Ellis, M. Czakon and S. Kirchner, *Two loop correction to interference in $gg \rightarrow ZZ$* , *JHEP* **08** (2016) 011
- [24] F. Caola, M. Dowling, K. Melnikov, R. Röntsch and L. Tancredi, *QCD corrections to vector boson pair production in gluon fusion including interference effects with off-shell Higgs at the LHC*, *JHEP* **07** (2016) 087.
- [25] R. Gröber, A. Maier and T. Rauh, *Top quark mass effects in $gg \rightarrow ZZ$ at two loops and off-shell Higgs boson interference*, *Phys. Rev. D* **100** (2019) 114013.
- [26] J. Davies, G. Mishima, M. Steinhauser and D. Wellmann, *$gg \rightarrow ZZ$: analytic two-loop results for the low- and high-energy regions*, *JHEP* **04** (2020) 024.
- [27] S. Alioli, S. Ferrario Ravasio, J. M. Lindert and R. Röntsch, *Four-lepton production in gluon fusion at NLO matched to parton showers*, *Eur. Phys. J. C* **81** (2021) no.8, 687 doi:10.1140/epjc/s10052-021-09470-5 [arXiv:2102.07783 [hep-ph]].
- [28] M. Grazzini, S. Kallweit, M. Wiesemann and J. Y. Yook, *Four lepton production in gluon fusion: Off-shell Higgs effects in NLO QCD*, *Phys. Lett. B* **819** (2021) 136465.
- [29] L. Buonocore, G. Koole, D. Lombardi, L. Rottoli, M. Wiesemann and G. Zanderighi, *ZZ production at n NNLO+PS with Mi NNLO_{PS}*, *JHEP* **01** (2022) 072.
- [30] U. Haisch and G. Koole, *Probing Higgs portals with matrix-element based kinematic discriminants in $ZZ \rightarrow 4\ell$ production*, *JHEP* **04** (2022) 166
- [31] B. A. Kniehl, *Radiative corrections for $H \rightarrow ZZ$ in the standard model*, *Nucl. Phys. B* **352** (1991) 1.

- [32] D. Pierce and A. Papadopoulos, *Radiative corrections to the Higgs boson decay rate Gamma ($H \rightarrow ZZ$) in the minimal supersymmetric model*, *Phys. Rev. D* **47** (1993) 222.
- [33] W. Hollik and J. H. Zhang, *Radiative Corrections to $H^0 \rightarrow WW/ZZ$ in the MSSM*, *Phys. Rev. D* **84** (2011) 055022.
- [34] S. Boselli, C. M. Carloni Calame, G. Montagna, O. Nicrosini and F. Piccinini, *Higgs boson decay into four leptons at NLOPS electroweak accuracy*, *JHEP* **06** (2015) 023.
- [35] A. Bredenstein, A. Denner, S. Dittmaier and M. M. Weber, *Precise predictions for the Higgs-boson decay $H \rightarrow WW/ZZ \rightarrow 4$ leptons*, *Phys. Rev. D* **74** (2006) 013004.
- [36] A. Bredenstein, A. Denner, S. Dittmaier and M. M. Weber, *Radiative corrections to the semileptonic and hadronic Higgs-boson decays $H \rightarrow WW/ZZ \rightarrow 4$ fermions*, *JHEP* **02** (2007) 080.
- [37] S. Liebler, G. Moortgat-Pick and G. Weiglein, *Off-shell effects in Higgs processes at a linear collider and implications for the LHC*, *JHEP* **06** (2015) 093.
- [38] B. Yan, *Determining Higgs boson width at electron-positron colliders*, *Phys. Lett. B* **822** (2021), 136709 doi:10.1016/j.physletb.2021.136709 [arXiv:2105.04530 [hep-ph]].
- [39] H. H. Patel, *Package-X: A Mathematica package for the analytic calculation of one-loop integrals*, *Comput. Phys. Commun.* **197** (2015) 276.
- [40] A. Denner and S. Dittmaier, *Reduction schemes for one-loop tensor integrals*, *Nucl. Phys. B* **734** (2006) 62.
- [41] T. Hahn and M. Perez-Victoria, *Automatized one loop calculations in four-dimensions and D-dimensions*, *Comput. Phys. Commun.* **118** (1999) 153.
- [42] N. Kauer and G. Passarino, *Inadequacy of zero-width approximation for a light Higgs boson signal*, *JHEP* **08** (2012) 116.
- [43] K. i. Hikasa, *Heavy Higgs Production in e^+e^- and e^-e^- Collisions*, *Phys. Lett. B* **164** (1985) 385 [erratum: *Phys. Lett. B* **195** (1987) 623].
- [44] K. I. Aoki, Z. Hioki, M. Konuma, R. Kawabe and T. Muta, *Electroweak Theory. Framework of On-Shell Renormalization and Study of Higher Order Effects*, *Prog. Theor. Phys. Suppl.* **73** (1982) 1.
- [45] G. Altarelli, B. Mele and F. Pitolli, *Heavy Higgs Production at Future Colliders*, *Nucl. Phys. B* **287** (1987) 205.
- [46] K. H. Phan and D. T. Tran, *One-loop Form Factors for $H \rightarrow \gamma^* \gamma^*$ in R_ξ Gauge*, *Comm. Phys.* **32** (2022) 77.
- [47] D. T. Tran and K. H. Phan, *One-loop formulas for $H \rightarrow Z\nu_l \bar{\nu}_l$ for $l = e, \mu, \tau$ in 't Hooft-Veltman gauge*, *Chinese Physics C* **47** (2023) 053106.

Appendix A: Checks for the calculation

Table 1. Checking for the UV-finiteness of the results at $M_{ZZ} = 250$ GeV ($p^2 = M_{ZZ}^2$). In this case, two real bosons are considered in final state.

(C_{UV}, μ^2)	$\sum_{j=1}^3 F_{00}^{(G_j)}$ $F_{00}^{(G_0)}$ $F_{00} = \sum_{j=0}^3 F_{00}^{(G_j)}$
(0, 1)	$-13.315051817147474 + 2.5760460657959703 i$ $16.425138633496918 + 0 i$ $3.110086816349444 + 2.5760460657959703 i$
$(10^2, 10^4)$	$137.93892691326275 + 2.5760460657959703 i$ $-134.82884009691335 + 0 i$ $3.110086816349394 + 2.5760460657959703 i$
$(10^4, 10^8)$	$13861.982684608432 + 2.5760460657959703 i$ $-13858.872597792075 + 0 i$ $3.1100868163575797 + 2.5760460657959703 i$

Before representing the phenomenological results, we are going to check the UV -finiteness of the results. As we mentioned in the previous section, the form factors $F_{00}^{(G_j)}$ for $j = 1, 2, 3$ contain the UV -divergent. By taking the counter-term form factor $F_{00}^{(G_0)}$, the total form factor F_{00} is then UV -finite. The numerical results for this check are presented in the following Table 1. By changing C_{UV}, μ^2 , we verify that the total form factor F_{00} is very good stability (over 11 digits).

Appendix B: Decay width of off-shell $H^* \rightarrow ZZ^* \rightarrow Zl\bar{l}$ and $H^* \rightarrow Z^*Z^* \rightarrow l_1\bar{l}_1l_2\bar{l}_2$ with $l_{1,2} = e, \mu, \nu_e, \nu_\mu, \nu_\tau$

We also include the leptons decay from Z boson. Since we are interested in the off-shell Higgs decay to ZZ . It means that $p_H^2 \geq 4M_Z^2$. Consequently, one can apply resonant approximation. The decay rates for $H \rightarrow ZZ^* \rightarrow Zl\bar{l}$ can be then presented in a compact form as:

$$\begin{aligned} \Gamma_{H \rightarrow Z^*Z \rightarrow Zl\bar{l}} &= \int_{4m_l^2}^{(M_{ZZ}-M_Z)^2} \frac{dq_1^2}{\pi} \frac{M_Z \Gamma_Z^l}{(q_1^2 - M_Z^2)^2 + M_Z^2 \Gamma_Z^2} \frac{g_{HZZ}^2 \sqrt{\lambda(M_{ZZ}^2, q_1^2, M_Z^2)}}{(64\pi) M_Z^3 M_{ZZ}^3 q_1^2} \\ &\times \left\{ \left[M_Z^4 - 2M_Z^2(M_{ZZ}^2 - 5q_1^2) + (M_{ZZ}^2 - q_1^2)^2 \right] \right. \\ &\quad + \left[2M_Z^4 - 4M_Z^2(M_{ZZ}^2 - 5q_1^2) + 2(M_{ZZ}^2 - q_1^2)^2 \right] \mathcal{R}e \left[F_{00}(M_{ZZ}^2, q_1^2, M_Z^2) \right] \\ &\quad \left. - \left(M_Z^2 - M_{ZZ}^2 + q_1^2 \right) \times \left[M_Z^4 - 2M_Z^2(M_{ZZ}^2 + q_1^2) + (M_{ZZ}^2 - q_1^2)^2 \right] \mathcal{R}e \left[F_{21}(M_{ZZ}^2, q_1^2, M_Z^2) \right] \right\}. \end{aligned} \quad (25)$$

Where $M_Z \Gamma_Z^l = \frac{M_Z g^2 s_W^2 (a_l^2 + v_l^2)}{12\pi}$ is partial decay rate of Z to lepton pair with $a_l = T_3^f / (2s_W c_W)$ and $v_l = (T_3^f - 2Q_f s_W^2) / (2s_W c_W)$. Following zero width approximation (ZWA) for Z decay into leptons, we employ

$$\frac{1}{(q_1^2 - M_Z^2)^2 + M_Z^2 \Gamma_Z^2} \rightarrow \frac{\pi}{M_Z \Gamma_Z} \delta(q_1^2 - M_Z^2). \quad (26)$$

One then has

$$\int_{4m_l^2}^{(M_{ZZ}-M_Z)^2} dq_1^2 \delta(q_1^2 - M_Z^2) = 1. \quad (27)$$

As a result, we arrive at

$$\Gamma_{H \rightarrow Z^*Z \rightarrow Zl\bar{l}} = \Gamma_{H \rightarrow ZZ} \times \text{BR}_{Z \rightarrow l\bar{l}}. \quad (28)$$

We next consider leptons decay from both Z bosons. Applying the resonant approximation, one-loop off-shell decay rates $H^* \rightarrow Z^*Z^* \rightarrow l_1\bar{l}_1l_2\bar{l}_2$ read:

$$\begin{aligned}
& \Gamma_{H \rightarrow Z^*Z^* \rightarrow 4 \text{ leptons}} = \tag{29} \\
& = \int_{4m_{l_1}^2}^{M_{ZZ}^2} \frac{dq_1^2}{\pi} \frac{M_Z \Gamma_Z^{l_1}}{(q_1^2 - M_Z^2)^2 + M_Z^2 \Gamma_Z^2} \int_{4m_{l_2}^2}^{(M_{ZZ} - \sqrt{q_1^2})^2} \frac{dq_2^2}{\pi} \frac{M_Z \Gamma_Z^{l_2}}{(q_2^2 - M_Z^2)^2 + M_Z^2 \Gamma_Z^2} \\
& \quad \times \frac{g_{HZZ}^2 \sqrt{\lambda(M_{ZZ}^2, q_1^2, q_2^2)}}{(64\pi) M_Z^2 M_{ZZ}^3 q_1^2 q_2^2} \left\{ \left[M_{ZZ}^4 - 2M_{ZZ}^2(q_1^2 + q_2^2) + q_1^4 + 10q_1^2 q_2^2 + q_2^4 \right] \right. \\
& \quad + \left[2M_{ZZ}^4 - 4M_{ZZ}^2(q_1^2 + q_2^2) + 2q_1^4 + 20q_1^2 q_2^2 + 2q_2^4 \right] \mathcal{R}e \left[F_{00}(M_{ZZ}^2, q_1^2, q_2^2) \right] \\
& \quad \left. + \left(M_{ZZ}^2 - q_1^2 - q_2^2 \right) \times \left[M_{ZZ}^4 - 2M_{ZZ}^2(q_1^2 + q_2^2) + (q_1^2 - q_2^2)^2 \right] \mathcal{R}e \left[F_{21}(M_{ZZ}^2, q_1^2, q_2^2) \right] \right\}.
\end{aligned}$$

With the help of ZWA, we arrive at

$$\Gamma_{H \rightarrow Z^*Z^* \rightarrow Zl_1\bar{l}_1l_2\bar{l}_2} = \Gamma_{H \rightarrow ZZ} \times \text{Br}_{Z \rightarrow l_1\bar{l}_1} \times \text{Br}_{Z \rightarrow l_2\bar{l}_2}. \tag{30}$$

Appendix C: Counter-term for the vertex HZZ

Counter-term for the HZZ vertex has general form as follows [44]:

$$F_{00}^{(G_0)}(p^2; q_1^2, q_2^2) = (\delta Y + \delta G_2 + \delta G_3 + \delta G_Z + 2\delta Z_{ZZ}^{1/2} + \delta Z_H^{1/2}) \langle ZZH \rangle, \tag{31}$$

where $\langle ZZH \rangle$ will refer to the tree-level expression of the above vertex. All renormalization constants can be found in [44, 47].

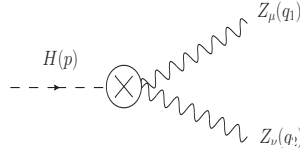


Fig. 5. Group 0: counter-term Feynman diagram.

Appendix D: Feynman diagrams

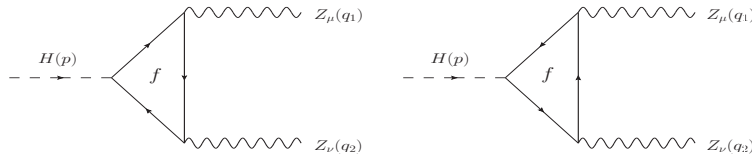


Fig. 6. one-loop Feynman diagrams with exchanging f in the loop (Group 1).

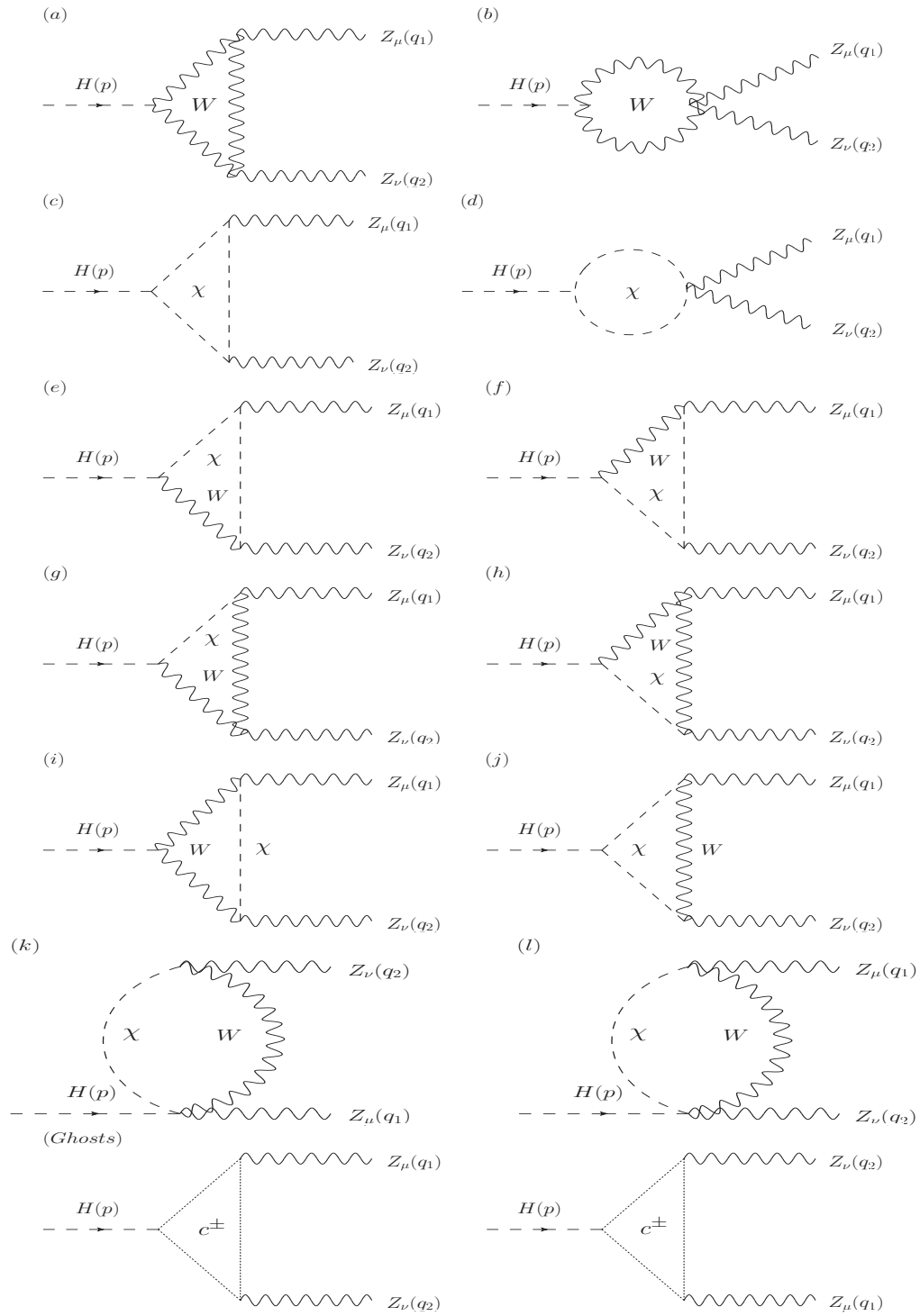


Fig. 7. one-loop Feynman diagrams with exchanging W, χ and ghost particles in the loop (Group 2).

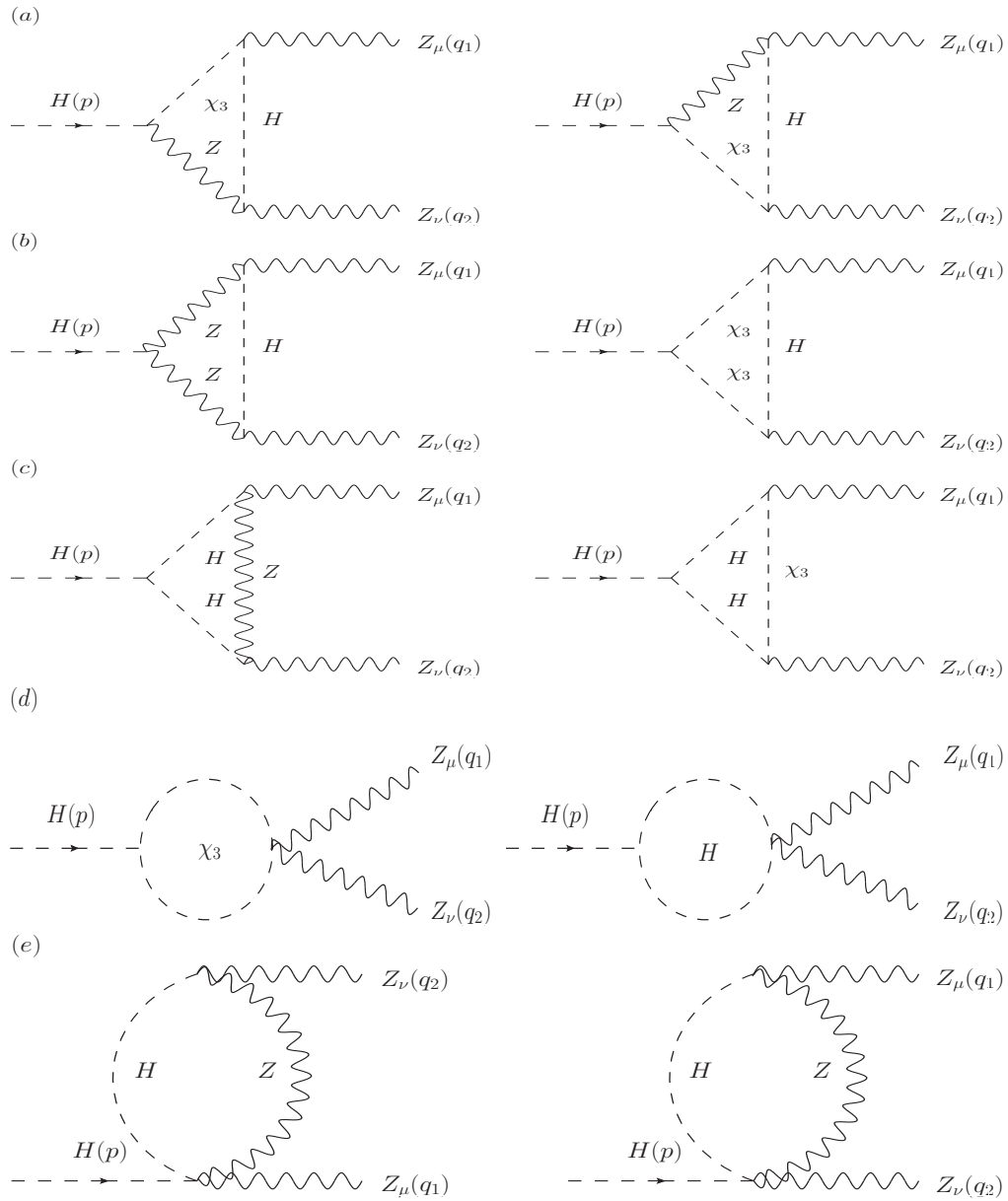


Fig. 8. one-loop Feynman diagrams with exchanging Z, χ_3 and H in the loop (Group 3).